Laser driven plasma accelerators

Francis F. Chen

Electrical Engineering Department, University of California
Los Angeles, California 90024

ABSTRACT

Linear particle accelerators can be made 100-1000 times shorter than conventional ones if the electric field of an electron plasma wave is used instead of that of a microwave cavity. Intense plasma waves can be excited by particle beams or laser beams. The most advanced concept, the Beat-wave Accelerator, has been studied extensively in theory, simulation, and experiment. Small-scale experiments have already demonstrated fields of order 1GeV/m, the existence of accelerated electrons, the effects of competing processes, and the nature of wave saturation. A proof-of-principle experiment employing a subnanosecond CO_2 laser is in progress.

1. INTRODUCTION

When intense laser pulses impinge on a solid target, large numbers of hyperthermal electrons are usually observed. Computer simulations have shown that these electrons are accelerated by plasma waves excited by either parametric instabilities or resonance absorption. One can make use of this strong effect by purposefully generating large-amplitude waves with relativistic velocities in a gaseous plasma using either laser or particle beams. The electric fields in such waves can exceed those in microwave cavities by a factor of order 10^3, so that linear accelerators for electrons or positrons can possibly be made shorter by this factor. Though the prospect of multi-TeV $e^+ - e^-$ colliders of lengths measured in meters instead of kilometers is attractive, a more realistic near-term objective would be the production of ultrashort GeV electron bunches that could produce femtosecond pulses of e.m. radiation. Various methods for wave excitation have been given in a more extensive review article[1]; in this paper, we summarize the results for the most highly developed laser-driven concept, the Beat-wave Accelerator[2] (BWA), and its variant, the Surfatron[3].

2. BEAT-WAVE ACCELERATOR

2.1. Fundamental relations

Two electromagnetic waves (ω_0, $\underline{k}_0$) and (ω_2, $\underline{k}_2$) will have a beat pattern whose ponderomotive force can excite a lower-frequency electrostatic wave (ω_1, $\underline{k}_1$) obeying the relations

$$\omega_0 = \omega_1 + \omega_2 , \quad \underline{k}_0 = \underline{k}_1 + \underline{k}_2 . \tag{1}$$

If $\underline{k}_1$ and $\underline{k}_2$ are directed oppositely, $|k_1|$ is large, and the phase velocity ω_1/k_1 is too small to be useful for acceleration to GeV energies. If $\underline{k}_0$ and $\underline{k}_2$ are co-directional, fast plasma waves are excited with

$$\omega_1 = \omega_0 - \omega_2 \equiv \Delta\omega \cong \omega_p \tag{2}$$

$$k_1 = k_0 - k_2 \equiv \Delta k \equiv k_p . \tag{3}$$

The phase velocity $v_p \equiv \omega_1/k_1$ is seen to be equal to the group velocity of the light waves $v_g = d\omega/dk \cong \Delta\omega/\Delta k$ in the limit $\omega_p \ll \omega_0$:

$$v_p \cong v_g = c(1 - n/n_c)^{1/2} \cong c , \tag{4}$$

where

$$n/n_c \equiv \omega_p^2/\omega_0^2 , \quad \omega_p^2 \equiv 4\pi n_0 e^2/m . \tag{5}$$

Defining the relativistic parameters $\beta_p \equiv v_p/c$ and $\gamma_p = (1 - \beta_p^2)^{-1/2}$, we find from Eq. (4) the convenient relation

$$\gamma_p = [1 - (1 - n/n_c)]^{-1/2} = (n_c/n)^{1/2} = \omega_0/\omega_p . \tag{6}$$

The synchronism between v_ϕ and v_g ensures that particle bunches trapped in the plasma wave will travel with the light pulse over long distances. Figure 1 shows schematically the injection and acceleration of (positive) electrons in a typical two-frequency laser pulse 10 psec (3 mm) long, containing 30 plasma wavelengths. Short pulses are necessary to avoid ion motion, which would detune the density and also permit a number of instabilities to grow.

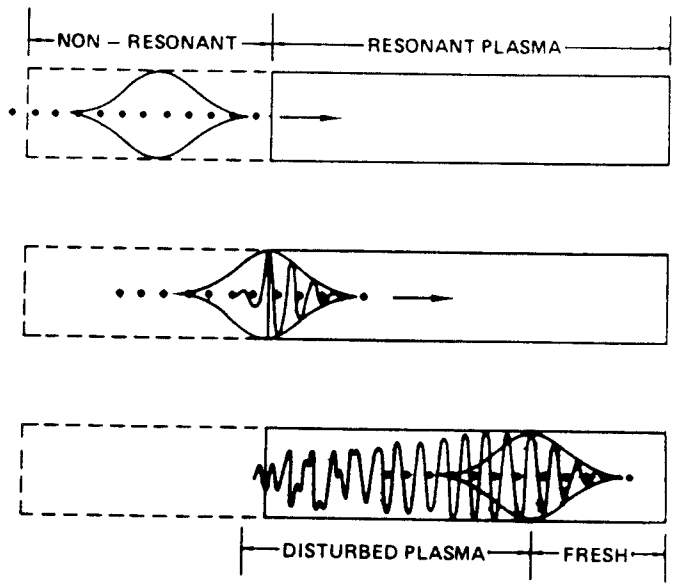

Fig. 1. Injection and acceleration of electrons in the BWA.

The *cold-plasma wave-breaking limit* is found from Poisson's equation $k^2\phi = 4\pi e n_1$ when the oscillating density is set equal to the background density n_0. Thus the maximum amplitude is

$$e\phi_{max} = 4\pi n_0 e^2/k_p^2 = m\omega_p^2/k_p^2 \cong mc^2 \tag{7}$$

for relativistic waves. Defining the relative amplitude

$$\varepsilon \equiv \phi/\phi_{max} = n_1/n_0 , \tag{8}$$

we find the plasma wave electric field to be

$$|E| = |k_p\phi| = \varepsilon k_p mc^2/e \cong \varepsilon\omega_p mc/e = 0.96\,\varepsilon n^{1/2} \ \text{V/cm} \tag{9}$$

Thus, the maximum accelerating gradient is $eE_{max} \cong 1$ GeV/m at $n = 10^{18}$ cm^{-3}. The value of n_0 is a compromise between large γ_p [Eq. (6)] and large E_{max} [Eq. (9)].

2.2. Beat-frequency excitation

Plasma wave excitation by optical mixing has been calculated by Rosenbluth and Liu[4] and confirmed in computer simulations[5]. The initial growth is linear at the rate

$$\partial\varepsilon/\partial t = \alpha_o\alpha_2\omega_p/4 \ , \qquad (10)$$

where

$$\alpha_j \equiv eE_j/m\omega_j c \ . \qquad (11)$$

As the oscillations grow, ω_p suffers a small redshift because of the relativistic increase in electron mass; and this detuning effect ultimately causes the waves to saturate at the level

$$\varepsilon_{sat} = (16\,\alpha_o\alpha_2/3)^{1/3} \ . \qquad (12)$$

The time τ to reach saturation, estimated from Eqs. (10) and (12), is given by

$$\omega_p\tau \cong 8(2/3)^{1/3}\,(\alpha_o\alpha_2)^{-2/3} \ , \qquad (13)$$

or $\tau \cong 8$ psec for $n_o = 10^{17}\,cm^{-3}$, $\alpha_o = \alpha_2 = 0.1$. Pulses longer than this would be counterproductive, giving rise to oscillations in the wave envelope because of excessive phase slip.

2.3. Particle acceleration

An electron trapped at $\phi = 0$ in a plasma wave of amplitude εmc^2 and falling to the bottom of the potential well will gain an energy $\Delta W \cong 2\varepsilon\gamma_p^2 mc^2$. One factor of γ_p arises from Lorentz contraction of the waves, and the other from the transformation of energy back to the laboratory frame. Let a particle (β, γ) have momentum $P = \gamma\beta mc$ and energy $W = \gamma mc^2$ in the laboratory frame and quantities β', γ', p', W' in the wave frame characterized by β_p, γ_p [Eq. (6)]. The Lorentz transformation

$$\begin{bmatrix} cp \\ iW \end{bmatrix} = \begin{bmatrix} \gamma_p & -i\beta_p\gamma_p \\ i\beta_p\gamma_p & \gamma_p \end{bmatrix} \begin{bmatrix} cp' \\ iW' \end{bmatrix} \qquad (14)$$

gives

$$W = \gamma_p\gamma'(1 + \beta_p\beta')\,mc^2 = \gamma mc^2 \ , \qquad (15)$$

or

$$\gamma = \gamma_p\gamma'(1 + \beta_p\beta') \ . \qquad (16)$$

Since $\underline{E}$ of the wave is parallel to $\underline{v}_p$, it remains invariant while $\phi = iE/k_p$ is increased by Lorentz contraction:

$$k_p' = k_p/\gamma_p \ , \quad \phi' = \gamma_p\phi \ . \qquad (17)$$

In the wave frame, an electron injected at $\phi' = 0$ can gain kinetic energy $e\phi'_{max} = \varepsilon\gamma_p mc^2$. Its total energy W' is then $\gamma' mc^2 = (1 + \varepsilon\gamma_p)mc^2$, or

$$\gamma' = 1 + \varepsilon\gamma_p \ , \quad \beta' = [1 - (1/\gamma'^2)]^{1/2} \ . \qquad (18)$$

Inserting γ' into Eq. (15) gives the energy in the laboratory, from which we must subtract the injection energy $\gamma_p mc^2$. Thus,

$$\Delta W = \gamma_p mc^2\,[(1 + \varepsilon\gamma_p)(1 + \beta_p\beta') - 1] \cong 2\varepsilon\gamma_p^2 mc^2 \qquad (19)$$

for the usual case $\beta_p \cong \beta' \cong 1$, $\varepsilon\gamma_p \gg 1$. For instance, $\varepsilon = 0.2$ and $\gamma_p = 100$ would give $\Delta W \cong 2$ GeV. The acceleration of positrons works equally well, but heavy ions would not be interesting because the energy gain is scaled to the electron mass.

Acceleration causes the particles to slip in phase relative to the plasma wave. When the particle reaches the bottom of the potential well, it must be ejected from the system. This occurs after an acceleration length L_a given by $\Delta W / E$, where $eE \equiv \varepsilon k_p mc^2$. Using Eq. (19) for ΔW, we find that ε cancels, and we have

$$L_a = 2\gamma_p^2/k_p = 2\gamma_p^2\,(c/\omega_o)\,(\omega_o/\omega_p) = 2\gamma_p^3/k_o \ . \qquad (20)$$

Thus, acceleration to large γ places stringent requirements on the production of uniform plasmas. Phase slip can be eliminated by tapering the density n_o or by using a magnetic field, but staging will in any case be dictated by practical considerations. In a staged accelerator, each section of length $L \equiv L_a$ has optimized n_o and γ_p and is the injector for the next section.

2.4. Injection, focusing, and beam loading

To trap a particle, a plasma wave must have amplitude $e\phi' = \gamma_p\varepsilon mc^2$ larger than the particle's kinetic energy $(\gamma' - 1)mc^2$ in the wave frame. In the usual case $\gamma_p \gg 1$, $\beta_p \cong 1$, this condition is approximately

$$\gamma > 2\varepsilon(1 + \varepsilon^2) \ . \qquad (21)$$

This condition is, however, modified by two-dimensional effects when the injected beam has finite emittance.

A radially varying plasma wave is shown schematically in Fig. 2. Such a wave has both a longitudinal component E_z and a radial component E_r, which is 90° out of phase. Particles must be injected in the quarter cycle in which E_z is accelerating and E_r is focusing.

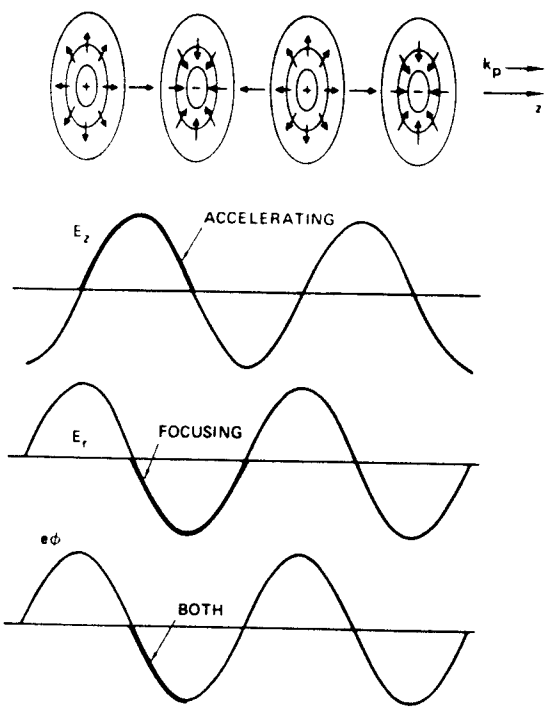

Fig. 2. Fields in a two-dimensional plasma wave.

To extract the maximum energy from the plasma waves, electron bunches injected at the right phase must also have the optimum density and shape factor. As shown by Wilks et al.[6], injected bunches should be triangular, with the highest density at the front (Fig. 3). This assures that the electric field within the

bunch is constant, so that all electrons are accelerated at the same rate. Each driven electron creates an electric-field wake which cancels the plasma wave behind it. If the maximum density in the bunch is of the order of the oscillating density in the wave, all of the energy of the wave can be given to the relativistic particles. However, the accelerating gradient in this case would be rather small. Fig. 4 shows a compromise case in which the gradient is 50% of the unloaded value and the wave loses 50% of its amplitude, or 75% of its energy.

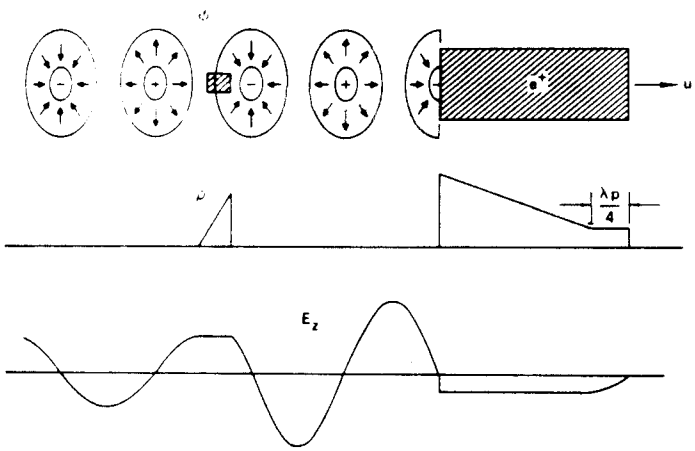

Fig. 3. A plasma wave loaded with an electron bunch with triangular density profile. In this case, the wave was created by another bunch rather than by laser beams.

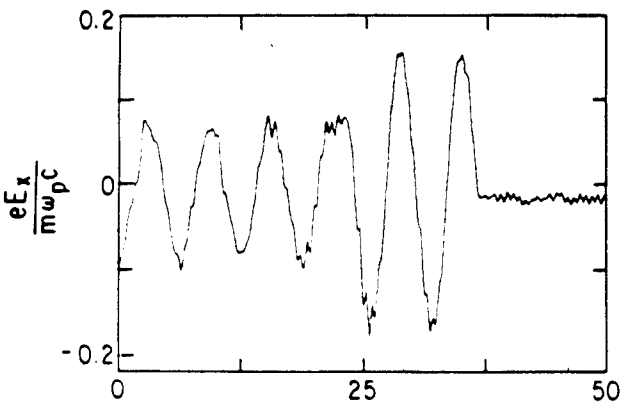

Fig. 4. One-dimensional simulation of a plasma wave loaded with an ideal triangular bunch with 75% efficiency. The bunch is located where the wake is flat-topped.

2.5. Efficiency, cascading, and staging

The **efficiency** of the BWA is the product of three efficiencies: (a) conversion of electrical power into laser light, (b) conversion of laser light into plasma waves, and (c) conversion of EPW energy into that of accelerated particles.

The laser efficiency (a) has not exceeded 5% in any existing short-pulse laser; but Nd-glass, CO_2, and excimer lasers could in principle achieve 10%. Of these, only the CO_2 laser can possibly be pulsed as rapidly as 1 kHz. Higher particle-beam luminosities may require the development of free-electron lasers with MHz repetition rates and $\geq$ 20% efficiencies.

The **beam-loading** efficiency (c) is less of a problem, though a compromise must be made with energy spread. As shown above, with proper shaping of the injected bunch, (c) can be $\geq$ 50%. The self-magnetic field of the accelerated beam and the beam's effect on the EPW frequency are questions yet to be addressed. The beat-wave efficiency (b) is a complex question which we now discuss.

The fundamental process in beat-wave excitation is the decay of blue photons $\hbar\omega_0$ into plasmons $\hbar\omega_p$ and red photons $\hbar\omega_2$. The efficiency is limited by the Manley-Rowe relation to ω_p/ω_0. This can be augmented by **cascading**, in which $\hbar\omega_2$ decays into $\hbar\omega_p$ and a redder photon $\hbar(\omega_2 - \omega_p)$, and so on until the light pulse reaches the end of the stage or a phase mismatch develops. (The k-mismatch due to light-wave dispersion can be shown, however, to be negligible under BWA conditions.) The subsequent decays continue to feed energy into the beat wave even after the original pumps have been depleted. This gain in conversion is offset by the fortunately weaker generation of higher frequency photons $\omega_n = \omega_0 + n\omega_p$ in the anti-Stokes process in which a plasmon is absorbed.

Cascading of the photons and the spreading of the light-wave spectrum, have been examined in the present context by Karttunen and Salomaa[7] for finite risetimes and collision frequencies. With dissipation, the beat-wave amplitude approaches a steady value, but for $KT_e > 100$ eV, collisions are too weak to prevent oscillation of the amplitude and sideband spectrum. Consider a square pulse just long enough to drive ε to ε_{sat} [Eq. (12)]. The pulse length L_p is approximately

$$L_p = 8.5 / (\alpha_o\alpha_2)^{2/3} k_p \ , \qquad (22)$$

and the conversion efficiency from photons to plasmons is

$$\eta_{bw} = (L/L_p)\,(16\alpha_o\alpha_2/3)^{2/3} / (\alpha_o^2 + \alpha_2^2)\,\gamma_p^2 \ , \qquad (23)$$

where the "stage length" L is the region over which useful plasma waves exist. Eq. (23) has a broad maximum near $\alpha_o = \alpha_2$. In that symmetric case, Eqs. (22) and (23) give

$$\eta_{bw} \cong 0.45\, k_p L \alpha_o^{2/3} / \gamma_p^2 \ . \qquad (24)$$

We may define the *depletion length* L_d to be the value of L for which $\eta_{bw} \cong 1$. We then have

$$k_p L_d \cong 2.2\, \gamma_p^2 / \alpha_o^{2/3} \ . \qquad (25)$$

Comparing this with the acceleration length $L_a = 2\gamma_p^2 / k_p$ [Eq. (20)], we see that

$$L_d/L_a \cong 1.1 / \alpha_o^{2/3} \ , \qquad (26)$$

which is larger than 1. It is therefore possible to make the stage length L as long as L_a without the necessity for replenishing the pump beams.

As an example, consider a stage in which $\varepsilon_{sat} = 0.2$ ($\alpha_o \cong 0.05$) and $\gamma_p^2 = 1000$ ($\Delta W = 200$MeV, $n_o = 1.2\times10^{15}$ cm^{-3} for CO_2 lasers). Then $L_a = 30$ cm, $L_d/L_a = 24$, and $\eta_{bw} = 0.9(L/L_a)\,\alpha_o^{2/3} = 0.12$ for $L = L_a$, as compared with the single-step Manley-Rowe efficiency of $\omega_o/\omega_p = \gamma_p^{-1} = .03$.

To keep the laser beams in focus, the stage length $L \equiv L_a$ should be less than the Rayleigh length

$$L_R = 2\pi w_o^2 / \lambda_o \quad . \tag{27}$$

Let the minimum waist size w_o be b times c/ω_p. Eq. (6) then gives

$$L_R = b^2 \gamma_p / k_p \quad . \tag{28}$$

Comparing this with $L_a = 2\gamma_p^2 / k_p$ [Eq. (23)], we see that $L_R/L_a = b^2/2\gamma_p$, which requires $b > (2\gamma_p)^{1/2}$.

To permit smaller radii, one can use relativistic self-focusing or hollow density profiles. The former comes about because electrons at the center of a Gaussian beam oscillate faster and are therefore heavier. This effect decreases ω_p and increases the index of refraction on axis, thus focusing the light, as verified in computer simulations by Forslund et al.[5]. The threshold for relativistic self-focusing depends on power rather than intensity, and is given by

$$P_{sf} \cong 10\,(\omega_o/\omega_p)^2 \text{ GW}. \tag{29}$$

For large γ_p, this threshold will not be reached, and one must keep the laser pulse focused by using an inverted density profile, which also acts as a positive lens. Because of the radial density gradient, the beat wave resonance is greatly modified. In the plasma fiber concept (Barnes et al.[8]), an electron density channel is created by the outward ponderomotive force of a single-frequency laser pulse, the ions being immobile. The channel traps the laser beam, acts as a slow-wave structure, an creates an axial component of $\underline{E}$ for acceleration.

2.6. Instabilities

In any plasma device, the possible instabilities must be examined carefully. The list below includes all instabilities known to be applicable to laser accelerators. Those which involve the slow motion of ions can be avoided by using short pulses, and those driven by particle beams can be suppressed by giving the beams a transverse energy spread[9]. No instability appears to be an insuperable obstacle, but for the BWA the most troublesome instability is likely to be stimulated Raman scattering (SRS).

Energy source	Electrons only	Ion motions also
Laser radiation	SRS modified SRS Compton scattering forward scattering relativistic self-modulation self-focusing filamentation	SBS modified SBS Compton scattering ponderomotive self-modulation self-focusing filamentation
Plasma wave	modulational instability (relativistic) resonant self-focusing (relativistic)	modulational instability (ponderomotive) resonant self-focusing (ponderomotive)
Particle beams	two-stream filamentation (Weibel) self-focusing (pinch) sausage and firehose	ion-acoustic (Buneman)

NONLINEAR PROPERTIES OF PLASMA WAVES

3.1 Nonlinear frequency shift

The Beat-wave Accelerator is sensitive to the nonlinear behavior of plasma waves. Perhaps the most fundamental point is the frequency shift at large amplitudes, a critical factor in the derivation of the Rosenbluth-Liu formula, Eq. (12). For nonrelativistic motions, Dawson[10] showed that the frequency ω_p is unchanged up to wave breaking; and for the relativistic case, Akhiezer and Polovin[11] showed that the only change is a redshift due to the mass increase. That all other nonlinearities cancel is, however, a subtle point which has only recently been clarified by McKinstrie and Forslund[12] and by Mori[13]. The source of discrepancies in the literature (referenced by the foregoing authors) lies in the dc component of the second order current $j^{(2)} = n_1 v_1 + n_o v^{(2)}$. Ampère's Law $c\,\underline{\nabla} \times \underline{B} = 4\pi \underline{j} + \partial \underline{E}/\partial t = 0$ shows that $j_{dc} = 0$ for electrostatic waves, so that the sum of $\langle n_1 v_1 \rangle$ and $n_o v_{dc}^{(2)}$ must vanish. If $v_{dc}^{(2)}$ is arbitrarily set equal to 0, a spurious blue shift is obtained due to the Doppler effect of $\langle n_1 v_1 \rangle$. There is, of course, a blue shift due to thermal motions in both the linear (Bohm-Gross) and nonlinear regimes.

3.2. Wavebreaking amplitude

As plasma waves become large, their wavefronts steepen until the electron fluid velocity v becomes comparable to the phase velocity v_p, and the particle positions become double-valued. This "wavebreaking" limit for cold, non-relativistic plasmas is given by Dawson[10] as

$$eE_{max}/m\omega_p v_p = 1 \quad , \tag{30}$$

which coincidentally agrees with the naive Equation (7) even though E_{max} and ϕ_{max} are no longer trivially related because of the development of harmonics. When finite T_e is introduced, E_{max} is reduced because the electron pressure resists compressions, and because thermally moving electrons are more easily trapped. The effect of relativity on plasma waves with $v_p \cong c$ is to increase E_{max} because the electrons become heavy ($v \cong c$) near wavebreaking and their orbits cannot easily overlap. Katsouleas and Mori[14] have recently calculated both thermal and relativistic effects. For $\alpha_t \equiv 3KT_e/mv_p^2 \ll 1$ and $\gamma_p \gg 1$, they obtain

$$eE_{max}/m\omega_p c = 2^{1/2}(2/5\alpha_t^{1/4} + 2\alpha_t^{1/4}/3 - \alpha_t/15 - 1)^{1/2}, \tag{31}$$

which is only 2.67 at $KT_e = 10$ eV. Though this value is larger than unity, even the latter may be unattainable because of instability limits.

3.3. Steepening, harmonics, and mode coupling

Since the equation of continuity for longitudinal waves gives $\underline{v}_1 = (n_1/n_o)\underline{v}_p$, there is a nonlinear effect causing electrons to move forward in the wave frame wherever $n_1 > 0$ and backward wherever $n_1 < 0$. This has the effect of bunching the density into striations and steepening the E-field sine wave into a sawtooth shape, thus generating harmonics in the ω and k spectra. Theoretical predictions on the growth of these harmonics have been confirmed in an experiment described in the next section.

Plasma accelerators, particularly the beat-wave accelerator, are sensitive to deviations from uniform density. In the BWA, an inhomogeneity in the form of a density ripple often arises because stimulated Brillouin scattering of either pump beam has a low threshold and excites an ion acoustic wave of typical amplitude $n_1/n_o = 1$ to 10%. For simplicity, we may assume the ion wave frequency to be essentially zero so that, from Eq. (1), the ripple is stationary with wave number $k_i = 2k_o$. The plasma wave is then described by the equation

$$\left[\frac{\partial^2}{\partial t^2} + \omega_p^2(z) - 3v_e^2\frac{\partial^2}{\partial z^2}\right]n_1 = C\,E_o E_2\ , \qquad (32)$$

where $v_e^2 = 3KT_e/m$, C is a coupling coefficient, E_o and E_2 are light waves, and $\omega_p^2(z)$ has the form $\omega_p^2(z) = \omega_{po}^2(1+\epsilon_i \cos 2k_o z)$. This equation was solved by Kaw etal.[15] for the undriven case $C = 0$, by Darrow etal.[16] for the beat-wave case with E_o and E_2 given, and by Barr and Chen[17] for the stimulated Raman instability, where E_o is a pump but E_2 is driven and follows a similar coupled equation.

In all cases the effect of the ripple is to couple energy from the fundamental mode (ω_p, k_p) into other modes with $\omega = \omega_p$, $k_m = k_p \pm mk_i$. In the BWA where $\underline{k}_o$ and $\underline{k}_2$ are in the same direction, Eq. (3) gives $k_p \cong \omega_p/c \ll 2k_o$; hence, the coupled modes are slow waves in either direction with $|v_p| \cong \omega_p/k_i$. In Raman backscatter (which occurs as an undesired process in the BWA), $\underline{k}_o$ and $\underline{k}_2$ are in opposite directions, and $k_p \cong -2k_o - \omega_p/c \lesssim k_i$. In the case of relativistic plasma waves with $k_p \cong \omega_p/c = k_o/\gamma_p$, Darrow etal.[16] show that the coupled modes can cause the beat wave to saturate at a level below that predicted by relativistic detuning [Eq. (12)]. They find that mode coupling dominates at low intensities such that $\alpha_o\alpha_2 < [1.6\epsilon_i/f(T_e)]^{3/2}$, where $f(T_e)$ is of order unity.

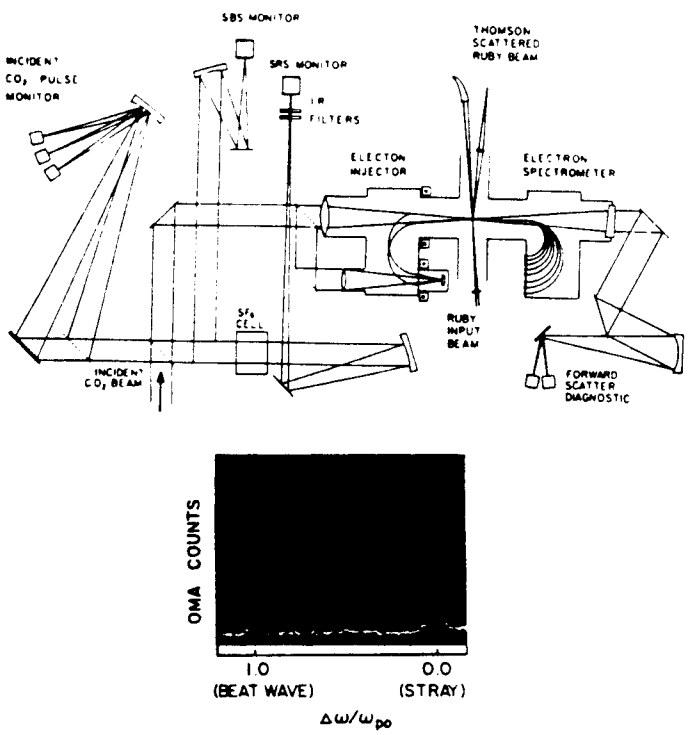

Fig. 5. Experimental arrangement of Clayton et al. (Ref. 18) and (below) signature of beat wave detected by Thomson scattering.

4. EXPERIMENTAL RESULTS

Experiments on the BWA concept are being carried out at the University of California, Los Angeles; at INRS-ENERGIE in Quebec, Canada; at the Rutherford-Appleton Laboratory in England; and the Institute of Laser Engineering in Osaka, Japan. In 1985, Clayton et al.[18] of the UCLA group, using the 9.6 and 10.6 μm lines of the CO_2 laser in the arrangement shown in Fig. 5, excited a relativistic plasma wave ($\gamma_p = 10$) over a 2-mm length and measured its amplitude by ruby laser scattering. With $\alpha_o = .017$ and $\alpha_2 = .034$, the results indicated $\epsilon \cong 3\%$, or $E_z \cong 1$ GV/m, which is consistent with Eq. (12) when modified for finite risetime (Forslund et al.[5]). Martin et al.[19] of the Canadian group, also using CO_2, have detected MeV electrons in a beat-wave experiment, but without direct confirmation of their origin. Danger etal.[20] of the British group attempted to beat 1 μm beams from a Nd-YAG laser, but encountered an unfortunate resonance with Raman scatter from atmospheric nitrogen. Nonetheless, they obtained interesting results on the production of uniform plasmas by multiphoton ionization.

Other experiments using essentially the apparatus of Fig. 5 have verified some of the predictions concerning plasma waves in an accelerator environment. Mode-coupling caused by the presence of ion waves created by Brillouin scatter has been seen by Darrow et al.[16]. Their data, shown in Fig. 6, indicate that the various modes are individually identifiable and do not cause the plasma to become completely turbulent.

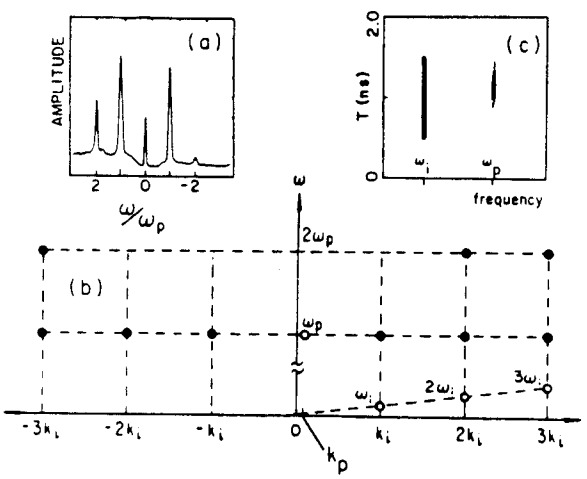

Fig. 6. Electrostatic modes observed by Thomson scattering in the beat-wave experiment of Darrow et al. (Ref. 16). The desired beat wave is at (ω_p, k_p). Open circles indicate scattering from ion waves and their harmonics. Modes at $(\omega_p, k_p \pm mk_i)$ are due to mode coupling. Modes at $(2\omega_p, mk_i)$ are mode coupled from plasma wave harmonics.

The generation of harmonics has been confirmed by Umstadter et al.[21] in plasma waves generated by SRS. Fig. 7 shows the observed amplitudes of the 2nd and 3rd harmonics as functions of the amplitude of the fundamental. The data were obtained by ruby-laser Thomson scattering at three scattering angles, and there is reasonable agreement with theory.

Currently, a proof-of-principle experiment is being carried out by the UCLA group using a kilojoule CO_2 laser which is a replica of one module of the former Helios laser at Los Alamos.

The laser has been converted to produce tens of joules in hundreds of picoseconds at 9.6 and 10.3 μm. The plasma target is a fully ionized theta-pinch. A 1.5-MeV electron linac is used to provide the requisite rejection energy. Acceleration to >10 MeV is expected.

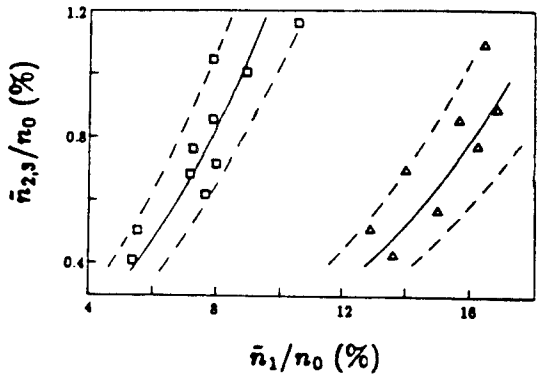

Fig. 7. Amplitudes of the harmonics n_2/n_o and n_3/n_o at $2\omega_p$, $2k_p$ and $3\omega_p$, $3k_p$, as functions of the fundamental amplitude n_1/n_o, measured experimentally by Umstadter et al. (Ref. 21). The lines are theoretical predictions, and the dashed limits reflect the error bars on n_1/n_o.

5. THE SURFATRON AND OTHER CONCEPTS

The phase slip of an accelerating particle in a plasma wave can be eliminated by the addition of a uniform, dc magnetic field $\underline{B}_o$. Arbitrarily long stage lengths are then possible, limited only by pump depletion. This method has been named the "surfatron" by Katsouleas and Dawson[3] and "v_p×B acceleration" by Sugihara et al.[22]. Consider the geometry of Fig. 8a, in which a particle being accelerated in a plasma wave with $\underline{v}_p$ in the x direction is subject to a field $\underline{B}_o$ in the z direction. The Lorentz force $F_y = -qv_xB_o/c$ gives the particle a velocity in the -y direction; and v_y, in turn, exerts a Lorentz force in the -x direction which prevents the particle from slipping forward in phase relative to the wave. Though the Lorentz force cannot give energy to the particle, it helps by keeping the particle at the position of maximum E_x. The particle is thus constrained to have $v_x = v_p$, but its γ can increase because its total velocity is at an angle $\theta = \tan^{-1}v_y/v_x$ (the "surfing angle") relative to the wave. This angle is shown in Fig. 8b, which also shows how a particle injected at an arbitrary phase will oscillate about its equilibrium position in the wave. These oscillations are damped as the particle approaches the light cone, partly because of conservation of action and partly because of its increase in mass. Therefore, in addition to unlimited acceleration, the surfatron offers the second advantage of a narrow energy spread.

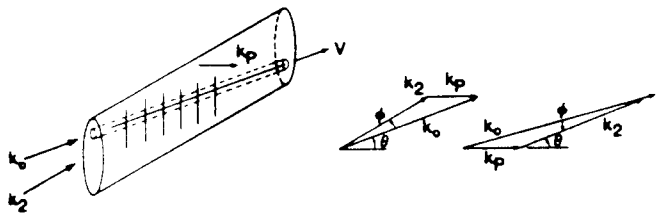

Fig. 9. Principle of finite-angle optical mixing.

In the wave frame moving with v_p, the field B_o transforms to $B_o' = \gamma_p B_o$, while the longitudinal field E_o is unchanged. The Lorentz force $F_x' = qv_yB_o'/c$ can never exceed the electrostatic force qE_o if $E_o > \gamma_pB_o$, since $v_y < c$. Thus, particles always remain trapped if $E_o > \gamma_pB_o$ or, from Eqs. (7) and (8), if $\omega_c < \varepsilon\omega_p/\gamma_p$. From the triangle in Fig. 8b, we see that $v_y = c(1-\beta_p)^{1/2} = c/\gamma_p$ after the particle reaches large γ, and therefore the angle θ is given by $\sin\theta \cong \theta \cong v_y/c = 1/\gamma_p$. From the relativistic theory given by Katsouleas and Dawson[3], the energy gain is $\Delta\gamma/\Delta x \cong \varepsilon k_p$. For example, to obtain 1 GeV electrons, one could beat CO_2 laser beams in a plasma of 10^{17} cm^{-3} density in a 20-kG magnetic field. One then has $\gamma_p = 10$ and $\theta = 5.7°$; and if $\varepsilon = 0.2$, $\Delta\gamma = 2000$ is reached in a distance $\Delta x = 17$ cm.

Since the particles move laterally a distance $\Delta y = 1.7$ cm in the above example, the plasma wave must have that width unless it can be made to follow the particle beam rather than the phase velocity $\underline{v}_p$. This can indeed be done by *finite-angle optical mixing*[23] of laser beams at an angle $\phi \cong \gamma_p^{-3}$. In Fig. 9 we show the vector relations which allow the beam $\underline{k}_o$ to follow the particle trajectories, which are at an angle θ to the plasma wave direction $\underline{k}_p$.

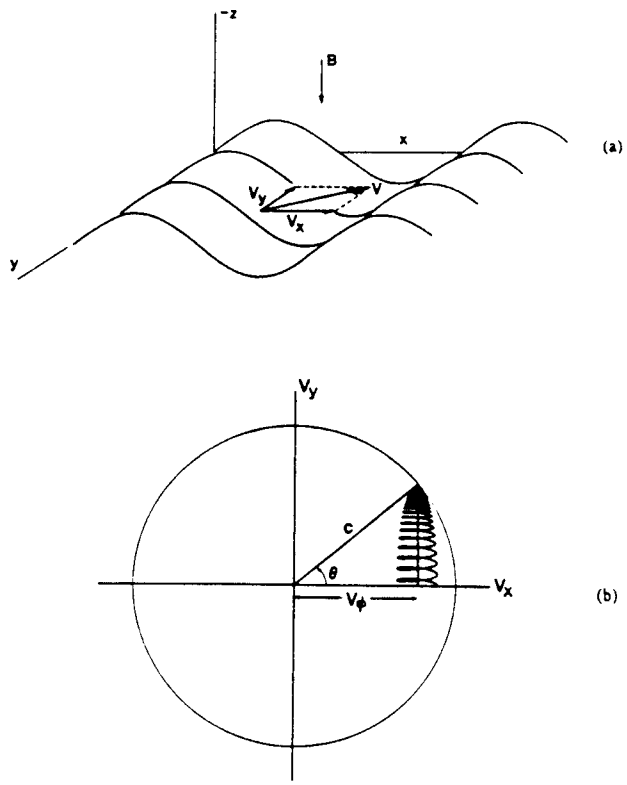

Fig. 8. (a) Geometry of the surfatron accelerator. (b) Particle trajectory in v_x - v_y phase space, showing damping of oscillations and surfing angle θ.

In the original work of Tajima and Dawson[24] a single laser pulse rather than a coherent EPW was envisioned. *Triple solitons* (Nishihara[25]) are pulses which can contain two beating laser beams and a plasma wave, phased in such a way as to leave no wake (Mima et al.[26]; McKinstrie and Dubois[27]). The energy of the EPW is given back to the light waves at the end of the pulse, thus increasing the pump depletion distance. However, loading was not considered.

Another solution to the pump depletion problem is to use *converging plasma waves* in which two beat waves are directed at an angle to the axis (Fig. 10). The interference pattern on the axis has a phase velocity faster than v_p which can be adjusted between stages to account for phase slip. Fig. 11 shows how the laser pulse might be replenished between stages. The *plasma waveguide* or *plasma fiber* accelerator (Barnes et al.[8]) is essentially the same idea, except that the EPW is a finite-geometry eigenmode with large $\omega/k_{||}$.

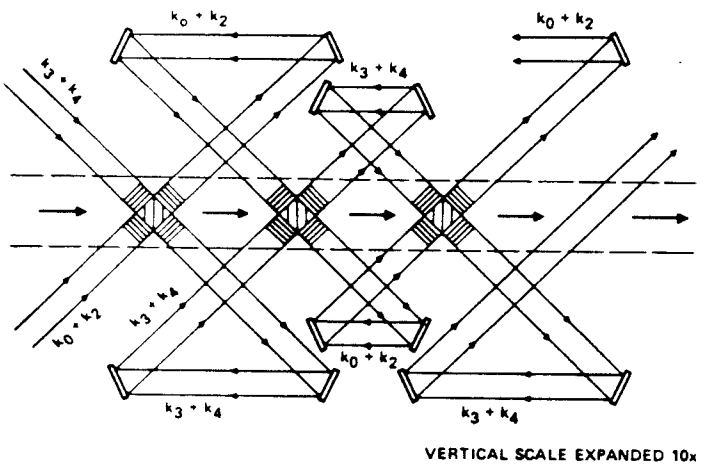

Fig. 10. Schematic of a converging plasma wave accelerator

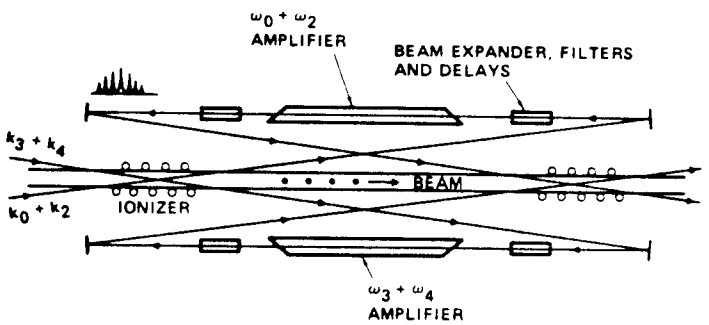

Fig. 11. A staged BWA with pump replenishment.

The *plasma grating accelerator* (Katsouleas et al.[28]) provides another way to generate EPW's of arbitrary phase velocity. Consider an ion acoustic wave (ω_i, k_i) propagating in the z direction and a laser beam (ω_o, k_o) propagating in the y direction with $\underline{E}$ in the z direction. The oscillating electrons in the laser beam will cause space charges to build up in the density ripple. The resulting electrostatic field has frequency $\omega \equiv \omega_o$ and $k \equiv k_i$ and can be decomposed into two counterpropagating plasma waves. This is essentially an oscillating two-stream instability seeded with an ion ripple.

6. ACKNOWLEDGMENTS

This work was supported by the National Science Foundation, Grant No. ECS83-10972 and by the Department of Energy, Contract No. DE-AS03-83-ER40120.

7. REFERENCES

1. F. F. Chen, "Laser Accelerators," in Physics of Laser Plasma, ed. by A. Rubenchik and S. Witkowski, Vol. 4 of Handbook of Plasma Physics, ed. by R. Z. Sagdeev and M. N. Rosenbluth (North Holland, Amsterdam, 1989); UCLA PPG-1107 (1987).

2. C. Joshi, W. B. Mori, T. Katsouleas, J. M. Dawson, J. M. Kindel, and D. W. Forslund, Nature **311**, 525 (1984).

3. T. Katsouleas and J. M. Dawson, Phys. Rev. Lett. **51**, 392 (1983).

4. M. N. Rosenbluth and C. S. Liu, Phys. Rev. Lett. **29**, 701 (1972).

5. D. W. Forslund, J. M. Kindel, W. B. Mori, C. Joshi, and J. M. Dawson, Phys. Rev. Lett. **54**, 558 (1985).

6. S. Wilks, T. Katsouleas, J. M. Dawson, P. Chen, and J. J. Su in IEEE Transactions of Plasma Science, ed. by T. Katsouleas, Vol. PS-15 (Institute of Electrical and Electronics Engineers, New York, 1987), 210.

7. S. J. Karttunen and R. R. E. Salomaa, Phys. Rev. Lett. **56**, 604 (1986).

8. D. C. Barnes, T. Kurki-Suonio, and T. Tajima, in: IEEE Trans. (loc. cit.), 154.

9. R. Bingham, W. B. Mori, and J. M. Dawson, in: Laser Acceleration of Particles, Malibu, California, 1984, ed. by C. Joshi and T. Katsouleas (Conference Proceedings No. 130, American Institute of Physics, New York, 1985), 138.

10. J. M. Dawson, Phys. Rev. **113**, 383 (1959).

11. A. I. Akhiezer and R. V. Polovin, Dokl. Akad. Nauk SSSR **102**, 919 (1955).

12. C. J. McKinstrie and D. W. Forslund, Phys. Fluids **30**, 904 (1987).

13. W. B. Mori, in: IEEE Trans. (loc. cit.), 88.

14. T. Katsouleas and W. B. Mori, UCLA Report PPG-1040 (1987).

15. P. K. Kaw, A. T. Lin, and J. M. Dawson, Phys. Fluids **16**, 1967 (1973).

16. C. Darrow, D. Umstadter, T. Katsouleas, W. B. Mori, C. E. Clayton, and C. Joshi, Phys. Rev. Lett. **56**, 2629 (1986).

17. H. C. Barr and F. F. Chen, Phys. Fluids **30**, 1180 (1987).

18. C. E. Clayton, C. Joshi, C. Darrow, and D. Umstadter, Phys. Rev. Lett. **54**, 2343 and **55**, 1652 (1985).

19. F. Martin, P. Brodeur, J. P. Matte, H. Pepin, and N. Ebrahim, in: IEEE Trans. (loc. cit), 167 and in: Advanced Accelerator Concepts, Madison, Wisconsin, 1986, ed. by F. E. Mills (Conference Proceedings No. 156, American Institute of Physics, New York, 1987), 112.

20. A. E. Dangor, A. K. L. Dymoke-Bradshaw, A. Dyson, T. Garvey, I. Mitchell, A. J. Cole, C. N. Danson, C. B. Edwards, and R. G. Evans, in: IEEE Trans. (loc. cit.), 161 and in: Advanced Accelerator Concepts 1987 (loc. cit.), 112.

21. D. Umstadter, R. Williams, C. Clayton, and C. Joshi, Phys. Rev. Lett. **59**, 292 (1987).

22. R. Sugihara, S. Takeuchi, K. Sakai, and M. Matsumoto, Phys. Rev. Lett. **52**, 1500 (1984).

23. F. F. Chen, Proc. XII Int'l Symposium on Physics of Ionized Gases, Sibenik, Yugoslavia, 1984 (World Scientific, Singapore, 1985), 937.

24. T. Tajima and J. M. Dawson, Phys. Rev. Lett. **43**, 267 (1979).

25. N. Nishihara, J. Phys. Soc. Japan **39**, 803 (1975).

26. K. Mima, T. Ohsuga, H. Takabe, K. Nishihara, T. Tajima, E. Zaidman, and W. Horton, Phys. Rev. Lett. **57**, 1421 (1986).

27. C. J. McKinstrie and D. F. DuBois, Phys. Rev. Lett. **57**, 2022 (1986).

28. T. Katsouleas, J. M. Dawson, D. Sultana, and Y. T. Yan, IEEE Trans. Nucl. Sci. **NS-32**, 3554 (1985).